SolarPACES 2023, 29th International Conference on Concentrating Solar Power, Thermal, and Chemical Energy Systems

Solar Industrial Process Heat and Thermal Desalination

https://doi.org/10.52825/solarpaces.v2i.789

Published: 24 Jul. 2024

Thermal Desalination Through Forward Osmosis Coupled With CO_2-Mixture Power Cycles for CSP Applications

Igor Matteo Carraretto[1], Ettore Morosini[1], Riccardo Simonetti[1], Marco Astolfi[1], Marco Binotti[1], and Giampaolo Manzolini[1]*

[1] Politecnico di Milano, Dipartimento di Energia, Via Lambruschini 4, 20156 Milano, Italy

* Correspondence: giampaolo.manzolini@polimi.it

Abstract. This work, performed in the framework of the H2020 EU project "DESOLINATION", analyses the coupling between CSP plants using transcritical power cycles with CO_2-mixtures and an innovative thermal desalination technique based on Forward Osmosis. Calculations are presented for a large scale CSP plant with central tower receiver and direct storage with solar salts in Dubai, adopting the mixtures CO_2+SO_2 and CO_2+C_6F_6 in the power cycles. The heat rejected from the cycle condenser is recovered directly by the FO plant, where the draw solute is heated up from 40 °C to 76 °C, to allow for the regeneration of the draw solution used in the forward osmosis membrane. The thermo-responsive polymer adopted is PAGB2000, already considered in literature as a promising option. Results show a very effective synergy between the electricity and the freshwater production: high yearly solar to electric efficiencies are possible (around 19%), with a low freshwater specific thermal consumption (around 100 kWh_{th}/m^3). The proposed desalination method is more effective than a conventional MED system (with + 50% of yearly freshwater produced), while a larger solar field (+ 28% in surface area) is necessary for a PV+RO plant to produce annually both the energy and freshwater produced by the CSP+FO plants.

Keywords: CO_2-Mixtures, Forward Osmosis, Thermal Desalination, CSP, Annual Analysis

Introduction

CO_2 mixtures adopted as working fluids in transcritical cycles for CSP applications have been demonstrated to be a promising solution to overcome the limits both of steam cycles characterized by low efficiency, high complexity and high cost of the power block, and of supercritical CO_2 cycles whose performance is penalized at high ambient air locations [1]. In fact, sCO_2 cycles are particularly efficient in a narrow range of cycle minimum temperatures, close to the fluid critical temperature (31 °C) where real gas effects and low fluid compressibility factor are exploited to reduce the compressor consumption. This is not generally possible for solarized power plants usually designed at cycle minimum temperatures above 50 °C to properly be coupled with air-cooling heat rejection units in hot climates. Alternatively, blending CO_2 with a dopant is considered a suitable approach to increase the critical temperature of the mixture working fluid, thus maintaining the compression process in the liquid region in any conditions and consequently increasing the cycle efficiency.

An additional advantage of CO_2 and CO_2 blended cycles with respect to steam cycles is the possibility to recover useful thermal power at temperatures up to 76 °C directly from the

heat rejection unit (HRU) without efficiency penalties related to working fluid bleeding from the turbine or to reduced pressure ratio due to backpressure at the turbine outlet. This mid temperature heat can be used to operate a seawater thermal-based desalination plant, operating with a sensible thermal source at low temperature. In the open literature, different works studied the integration of a multi effect distillation desalination plant with the sCO_2 power cycles, showing specific thermal consumptions around 150 kWh per cubic meter of desalinated water, if all the thermal power recovered from the HRU of the sCO_2 cycle is exploited [2]. This work, instead, focuses on forward osmosis (FO) as thermal desalination technique, to stress its lower specific thermal consumption with respect to the conventional solution [3].

This study has been carried out in the framework of the H2020 EU "DESOLINATION" project which aims at developing an innovative process exploiting Concentrated Solar Power (CSP) for production of both green electricity with a transcritical CO_2 blended cycle and freshwater through Forward Osmosis (FO) desalination. The schematic of the system under study is reported in Figure 1 and it encompasses three main sub-parts that are be presented in following sections: the solar plant is based on a central solar tower, a cylindrical external tubular receiver using solar salts up to 565 °C as heat transfer fluid [4], and a surrounded heliostat field. The solar section is oversized to collect more solar energy and extend the operating hours of the power block thanks to the introduction of a thermal energy storage system. The power block is based on transcritical CO_2 blended cycles and for this work two cases are investigated varying the dopant (SO_2 and C_6F_6) and adopting the most appropriate cycle configuration. Heat is provided to the cycle by cooling the solar salts taken from the hot tank and eventually stored in the low temperature tank. Finally, the desalination section receives heat released from the power block heat rejection unit (HRU) and produces fresh water through a forward osmosis process.

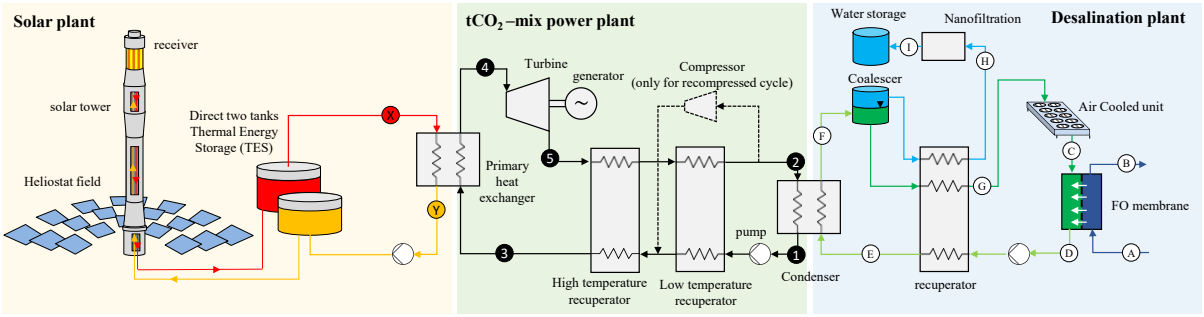

Figure 1. *Plant layout including solar power (yellow box), power plant (green box) and desalination plant (blue box).*

CSP plants definition: a case study in Dubai

The performances of the innovative plant are evaluated for a specific case study, choosing Dubai as location (DNI = 1755 kWh/m^2/year). The design of the CSP heliostat field and its optical performances are computed with SolarPilot [5]: considering a nominal DNI equal to 1000 W/m^2 at solar noon of the spring equinox and by setting the power hitting the receiver equal to 870 MW_{th}. Heliostats of 10 m x 10 m are adopted, while the HTF is conventional solar salt [4]. The HTF flows in two flowpaths in the receiver (E/W), with 4 panels per flowpath. The diameter of the tubes is 60.3 mm and their thickness 1.65 mm, taken from standard sizes [6]. The tubes emissivity and absorptivity are 94% and 87%, respectively [7]. The receiver aspect ratio is fixed at 1.25 and its diameter is computed to have a maximum solar flux of 1 MW_{th}/m^2 at design conditions, using image size priority with a maximum offset factor of two as heliostats aiming strategy. Tower height is fixed at 225 m.

The receiver HTF outlet temperature is fixed to 565 °C, while two different inlet temperatures, 390 °C and 425 °C, are considered for the two cycles simulated in this work assuming a ΔT of 20 °C at the cold end of the primary heat exchanger (see Table 3). The thermal efficiency of the receiver is computed with an in-house code [8] and the computed values for these two cases are very similar (relative difference lower than 0.33%) at both nominal and reduced heat flux (Figure 2 left). On the contrary the two cases remarkably differ in pressure drops (cf. Table 1) according to the different solar salt mass flow rate which in turn leads to different HTF pump electric consumption as function of the incident solar power. Figure 2 (right) shows details of both the monthly average DNI and the thermal energy collected for a representative year (2019).

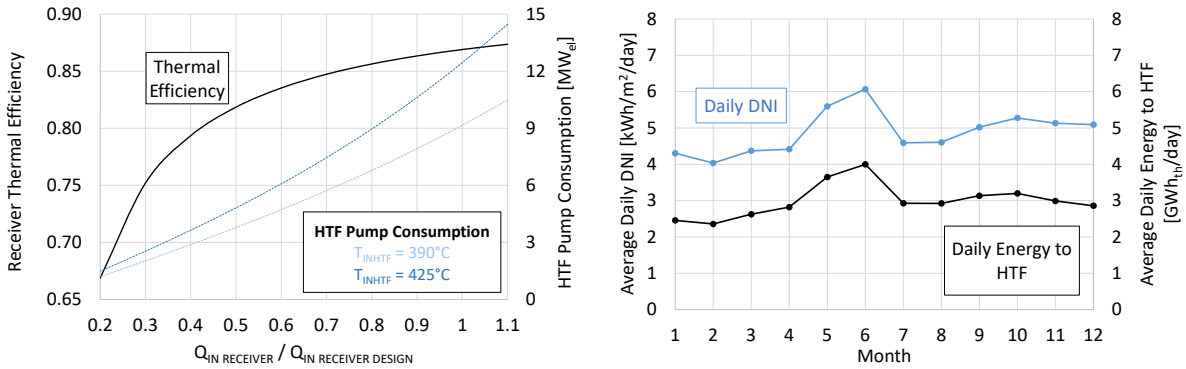

Figure 2. *Receiver off-design analysis (left), solar resources and energy produced (right).*

Table 1. *Solar field and receiver design results.*

Resulting characteristics	**Value**
Number of tubes per panels [-], spacing between tubes [mm]	120, 1.9
Receiver Height [m], Diameter [m]	23.8, 19
Heliostat number	14051
Optical and Thermal Efficiency at design	63.8%, 86.9%
Nominal power to HTF [MW_{th}]	760
HTF ΔP in the receiver with $T_{IN\ HTF}$ = 390 °C, 425 °C [bar]	7.6, 11.9
Nominal HTF mass flow rate with $T_{IN\ HTF}$ = 390 °C, 425 °C [kg/s]	2785, 3475
Nominal power of HTF pump with $T_{IN\ HTF}$ = 390 °C, 425 °C [MW_{el}]	9.2, 12.4

Modelling of tCO_2-mixtures cycles for solar applications coupled with FO

Two CO_2-based mixtures are considered for the case study in transcritical cycles: CO_2+C_6F_6 and CO_2+SO_2, whose effectiveness as working fluids in power cycles has been already demonstrated in previous literature works [7], [9]. Due to the different glide of the two mixtures during condensation, for the C_6F_6 mixture a simple recuperative cycle is adopted, while for the SO_2 mixture a recompressed cycle has been selected. The cycle schemes are reported in Figure 1 (green box) and the main difference is related to the use of an additional compressor in the recompressed cycle (CO_2+SO_2) that elaborates a fraction of the main mass flow rate to balance the heat capacities on the low temperature recuperator thus leading to lower temperature differences and a higher recuperative process effectiveness. Mixtures composition has been considered a degree of freedom, selected to maximize the cycle efficiency at design conditions for both mixtures.

Table 2 reports the assumptions adopted for the cycles design. Maximum temperature has been set considering a temperature difference of 15 °C at the primary heat exchanger

hot end while maximum pressure is pushed at the upper level usually adopted for sCO_2 studies, which represents the best tradeoff between cycle performance increase and issues related to components design. Minimum cycle temperature is set 6 °C higher than the expected draw solution return temperature from the recuperator of the desalination plant.

Table 2. *Assumptions on the cycle.*

Assumption on the cycle performance	**Value**
Maximum cycle temperature [°C], pressure [bar]	550, 250
Minimum cycle temperature [°C]	51
Isentropic efficiency of the expansion and compression	92%, 88%
Recuperators Minimum temperature difference [°C]	5
Pump inlet subcooling (Minimum pressure – Bubble pressure) [bar]	3
Pressure drops across PHE, PCHE LP, PCHE HP, Condenser [bar]	2, 1, 0.5, 1

The simulations of the two power cycles have been carried out in ASPEN Plus v.11 adopting the PC-SAFT Equation of State and binary interaction parameters as suggested in literature [10], [11]. Table 3 presents the cycles performance at design conditions while Figure 3 depicts the Temperature vs. Specific Entropy diagrams for the two selected thermodynamic cycles. The main difference is related to the pressure ratio that is higher for the CO_2+SO_2 cycle (3.20 vs. 2.88) because of the lower condensation pressure for the selected cycle minimum temperature and pump inlet subcooling degree. Therefore, the turbine outlet temperature (412 °C vs. 459 °C) and the primary heat exchanger temperature decrease (370 °C vs. 405 °C) leading to a higher HTF temperature variation and a lower HTF mass flow rate. As already highlighted in the previous section this translates in a lower HTF pump consumption that is around 26% lower with respect to the CO_2+C_6F_6 system. The lower turbine outlet temperature also causes a reduction of the recuperative section duty: in case of CO_2+SO_2 the heat recovered in the recuperator from hot working fluid released by the turbine is 174% of the heat input from HTF, while in case of CO_2+C_6F_6 this represents the 273%. The lower average temperature difference in the recuperative section is however lower for the recompressed cycle (CO_2+SO_2) thanks to a better heat capacity matching but the overall heat transfer area here quantified as UA parameter is still higher for the simple recuperative cycle working with CO_2+C_6F_6. Another difference concerns the low-pressure side recuperator outlet condition that in CO_2+C_6F_6 case drops in two phase flow region possibly leading to difficulties related to fluid distribution to the condenser and liquid phase slip if velocity in the connection piping is not sufficiently high. The cycle electric output, instead, is fixed at 100 MW_{el} for both configurations, resulting in a different thermal power released to the desalination plant at design.

Table 3. *Power cycles main thermodynamic performance parameters.*

Power cycle characteristic	**CO_2+SO_2 Cycle**	**CO_2+C_6F_6 Cycle**
Molar fraction of CO_2 in the mixture	76%	87%
Power block configuration	Recompressed	Recuperative
Electric cycle efficiency, Gross cycle efficiency	43.4%, 44.2%	41.5%, 42.1%
Cycle specific work [kJ/kg]	92.6	80
Power cycle electric output [MW_{el}]	100	100
Thermal power released to the FO desal. plant [MW_{th}]	129	141
Minimum cycle pressure [bar]	79	87
Compressor Pressure ratio [-]	3.20	2.88
Turbine outlet temperature [°C]	412	459
Primary heat exchanger inlet temperature [°C]	370	405
Recuperator duty [MW_{th}]	402	667
$UA_{Recuperators}$ [MW/K]	29.9	38.6
Temperature [°C] /Vapor quality at HRU inlet	85 / SH	81 / 69%mol.

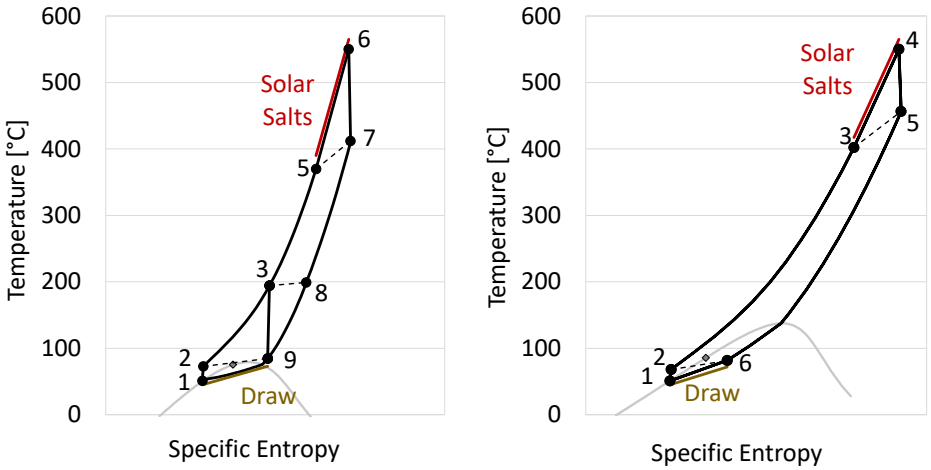

Figure 3. *Temperature vs. Specific Entropy diagrams for the two selected thermodynamic cycles: CO_2+SO_2 (left) and CO_2+C_6F_6 (right).*

Modelling of thermal desalination with forward osmosis

The thermal power released from the condenser of the power plant (Figure 1 green box), independently of the analysed cycle, is used to regenerate the draw solution of the Forward Osmosis process (Figure 1 blue box). The coupling between the power cycle and the desalination plant is designed to maximize the yearly water produced by recovering all the thermal power available at the condenser.

Polymer PAGB2000 has been adopted as draw solute in the desalination plan both due to its favorable thermo-responsive behavior [12] (Figure 4 depicts the Lower Critical Solution Temperature curve) and because it has been already identified in a previous campaign as promising for FO processes [3]. The FO plant is modelled with an in-house code previously developed and published in the open literature [3], updated including the polymer properties taken during an experimental campaign [13].

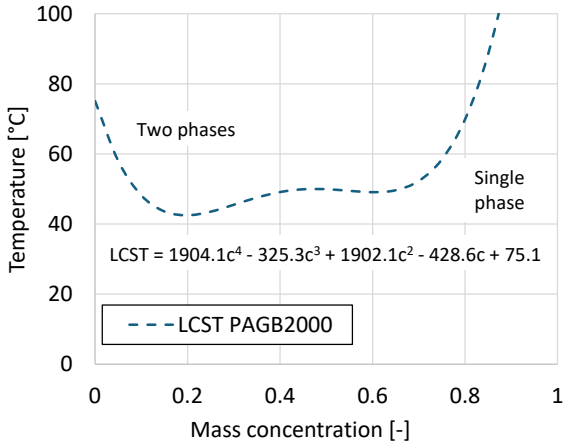

Figure 4. *Phase diagram of PAGB2000 according to experimental data reported in [13].*

The Forward Osmosis plant layout is reported in Figure 1 (blue box). The seawater (A-B) is pumped through the FO membrane (T_A = 25 °C), where it flows counter-current with respect to the highly concentrated polymeric solution (C-D) at c_C = 0.816 wt./wt. and T_C = 40 °C: the computed recovery ratio is 30%, necessary to have T_B < 37 °C. The diluted draw solution (D), at c_D = 0.65 wt./wt, leaves the FO membrane at a temperature very close to T_A. It

enters at first the recuperator and then the cycle condenser, at a temperature (T_E) of 45°C, to be heated up to 76 °C (F). The maximum temperature is set to effectively regenerate the draw solution according to LCST curve (cf. Figure 4). Then the two-phase mixture enters the coalescer (F), where the two phases are split in a polymer-rich (G) and a water-rich (H) stream. Both flows enter the recuperator: the polymer rich cools down to 63 °C and it is further cooled down in an air heat-rejection unit before being fed to the FO membrane, whereas the water rich one is cooled down in the recuperator at 44 °C to comply with the maximum allowable temperature of nanofiltration equal to 45 °C [3], and it is furtherly purified, obtaining fresh water through the nanofiltration. To avoid variable conditions at the interface between the cycle condenser and the FO plant, the power cycle is operated always at full load, always at fixed cycle minimum temperature of 51°C, whenever thermal power is available either from the solar receiver or the TES. At these conditions only 47% of the thermal input from the power block condenser of the cycle is rejected in the air cooler unit: the remaining 53% is dissipated in both the stored freshwater (I) and the heated brine (B).

The composition of the two flows at the outlet of the membrane (B and D) are found to maximize the plant performance, maintaining a positive difference of osmotic pressure across the two bulk flows of the membrane, to promote the mass transfer, without computing the membrane dimensions.

The two parameters of relevance to understand the performances of desalination process are the specific thermal and electric consumptions (with details on their modeling already discussed in literature [3]). The specific thermal consumption of the FO plant is related to the heat required to heat up the solution from T_E up to T_F:

$$Q_{th,spec} = m_E c_E (T_F - T_E)/V_{FRESH} \quad (1)$$

Accordingly, the thermal consumption decreases when T_F decreases (a limit that is set by capability of the solution to separate in two phases, depending only on the thermo-responsive characteristics of the draw) and when T_E increases, directly influencing the heat recovery from the power cycle HRU. An insight into the heat exchange process in the HRU is shown in *Figure 5* for both power cycles, ensuring a minimal internal temperature difference between the two flows of around 2 °C. In this configuration of the FO plant, the specific thermal consumption results equal to 100 kWh_{th}/m^3, thus being lower than the value for conventional Multi Effect Distillation (MED) which (for the same temperatures) shows thermal consumptions of 155 kWh_{th}/m^3.

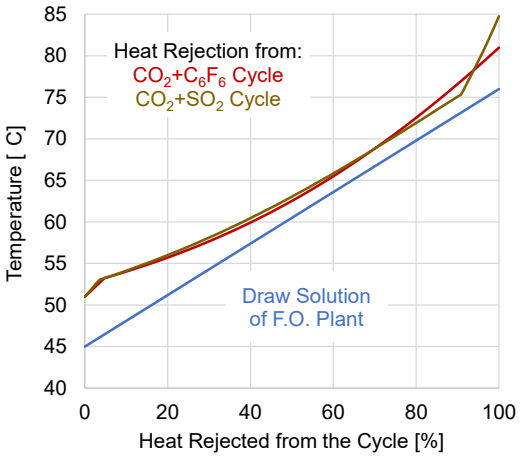

Figure 5. *T-Q diagrams of the two HRUs of this work, with T_F = 76 °C and T_E = 45 °C.*

The electric consumption of the FO plant, on the other hand, is much lower than for RO plants, and it is related to: (a) the pumping power required to overcome the pressure

losses along the circuit and within the components, (b) the pump consumption in the nanofiltration step (providing the overpressure necessary to perform the separation of the remaining polymer traces), and (c) the air-cooler electric consumption to cool down the concentrated draw solution before being re-injected in the membrane:

$$E_{el,\ spec} = (E_{el,pump} + E_{el,NF} + E_{el,air\text{-}cooler}) / V_{FRESH} \quad (2)$$

The pump and nanofiltration consumption are around 0.5 kWh_{el}/m^3 according to literature [3], while the consumption of the air cooler is computed assuming 100 Pa of air pressure drop at design and a 50% of electromechanical efficiency of the fan. At design conditions (35 °C of ambient temperature), the $E_{el,air\text{-}cooler}$ is around 400 kW_{el} (around 0.2 kWh_{el}/m^3) which leads to an overall electrical consumption of 0.7 kWh_{el}/m^3 which is much lower than the specific power required for Reverse Osmosis (RO) equal to 4 kWh_{el}/m^3 [3]).

Yearly results analysis and comparison against conventional solutions

The annual performance of the two plants located in Dubai has been evaluated adopting hourly based weather data (presented in Figure 2). Having fixed the electric power of the cycle at 100 MW_{el}, the TES size is varied to limit the defocused radiation to a level below 20 hours for both power cycles considered, resulting in 11 equivalent hours of TES size [14]. Fixing both the cycle net power at a reference value and the solar plant design, the resulting solar multiple (SM) is computed as 3.2 for the recompressed CO_2+SO_2 cycle and 3.1 for the simple CO_2+C_6F_6 cycle. On an hourly basis, the optical efficiency is computed in SolarPilot [5] and both the thermal efficiency and the parasitic electric losses of the HTF pump are evaluated as reported in Figure 2. On the contrary, the power block works always works in nominal conditions being condesated with diluted draw solution coming from the FO desalination plant at a constant temperature, independently of the ambient one. The results of the yearly analysis are proposed in Table 4, showing little differences between the two systems, mainly related to the different thermodynamic efficiency of the two cycles.

Table 4. *Results of the annual analysis of the CSP plants in Dubai.*

Power plant performance indicator	CO_2+SO_2 Cycle	CO_2+C_6F_6 Cycle
Yearly solar to electric efficiency	19.0%	18.0%
Yearly electric energy produced [GWh_{el}/year]	454	432
Capacity factor of the CSP plant	51.8%	49.3%
Yearly energy to the desalination plant [GWh_{th}/year]	599	623

The specific thermal and electric consumption of the FO plant, for the case study of this work, are equal to 100 kWh_{th}/m^3 and 0.7 kWh_{el}/m^3, respectively. While the first is constant the second one is variable considering that the pump and nanofiltration consumption are constant while the draw solution heat rejection unit fan consumption is computed on hourly base depending on the ambient temperature according to previous published methods [9].

The results of the coupling between the CSP and the FO plants are summarized in Table 5, both at design conditions and on annual basis in Dubai. The results of the FO plant are compared and benchmarked with two reference plants:

- A conventional MED system, simulated according to a MED model derived from literature [2] which results in a specific thermal consumption of 155 kWh_{th}/m^3 when heat is provided at the temperatures of the CO_2 blended cycle heat rejection process, in the same range of the FO plant (45 – 76°C). This consumption is constant and independent from weather data, as reported in literature.

- A desalination plant powered by PV and adopting a reverse osmosis (RO) system having an electric consumption of 4 kWh_{el}/m^3 [3]. For the PV plant, it is assumed an electric efficiency at Standard Test Conditions of 19.0% as for the default PV system in the SAM database. The assessment of the yearly performance of the PV system in Dubai, considering the same weather data considered for the CSP plant, is computed in SAM, assuming no tracking systems, panel tilt and azimuth angles of 30° and 180°, respectively. The PV plant net annual capacity factor results equal to 19.0%, including the temperature effects on the conversion efficiency and all the other conversion losses included by default in the tool.

Considering as key figure of merit the annual water production specific to the surface area of the heliostats, for the case-studies based on CSP the ones coupled with FO produce 50% more freshwater than the ones with MED, adopting the same power cycles and heat source for the desalination plant, denoting the very promising performances of FO as thermal desalination technology working with low temperature sensible heat. The specific energy production for the two CSP plants considered in this work is around 63 W_{el}/m^2 (per each square meter of heliostat aperture area at design conditions, including the HTF parasitic losses), while it is around 0.32 MWh_{el}/m^2 on annual basis.

Table 5. *Comparison of the specific freshwater production with CSP+FO and CSP+MED.*

Plant type	Working fluid	Design Results [liter/hour/$m^2_{Heliost.}$]	Yearly Results [m^3/year/$m^2_{Heliost.}$]
CSP + CO_2 Mix Cycle + MED	CO_2+C_6F_6 Mix	0.65	2.86
	CO_2+SO_2 Mix	0.60	2.75
CSP + CO_2 Mix Cycle + FO	CO_2+C_6F_6 Mix	0.99	4.36
	CO_2+SO_2 Mix	0.91	4.18

According to the previous results, the comparison against a PV+RO system is carried out only considering the CSP+FO plant adopting the mixture CO_2+SO_2 because of the more favorable cycle configuration and the higher cycle electrical efficiency. The calculations, for the PV+RO plant, are carried out computing the PV panels overall surface area that can produce yearly the same amount of both electric energy and freshwater of the CSP+FO, proposed in Table 6.

Table 6. *Solar field area comparison between CSP+FO and PV+RO.*

	CSP+FO system	PV+RO system (with storage)
Annual Electricity production [GWh_{el}/year]	454	
Annual freshwater production [m^3/year]	$5.87 \cdot 10^6$	
Solar field area [m^2]	1 405 100 (Heliostats)	1 795 100 (PV panels)
Dispatchability factor	38%	

Overall, for the same yearly energy and freshwater production an increase by + 28% in the solar field area is expected for the PV+RO technology, with respect to the innovative CSP+FO cogenerative system. This difference is shown in *Figure 6* by the Sankey diagram of the energy balance for the CSP+FO plant adopting CO_2+SO_2 mixture, as working fluid in the power cycle, and the PV+RO case, equipped with electrochemical batteries able to provide the system with the same dispatchability level of the CSP plant, assuming standard lithium-ion batteries for stationary applications with an efficiency of 59.5% according to [15]. In this work the dispatchability factor is defined as the yearly energy delivered to the power block from TES with respect to the overall yearly value. This is a very conservative assumptions

combined with the site selection with is characterized by low DNI and high diffuse radiation favouring PV technology.

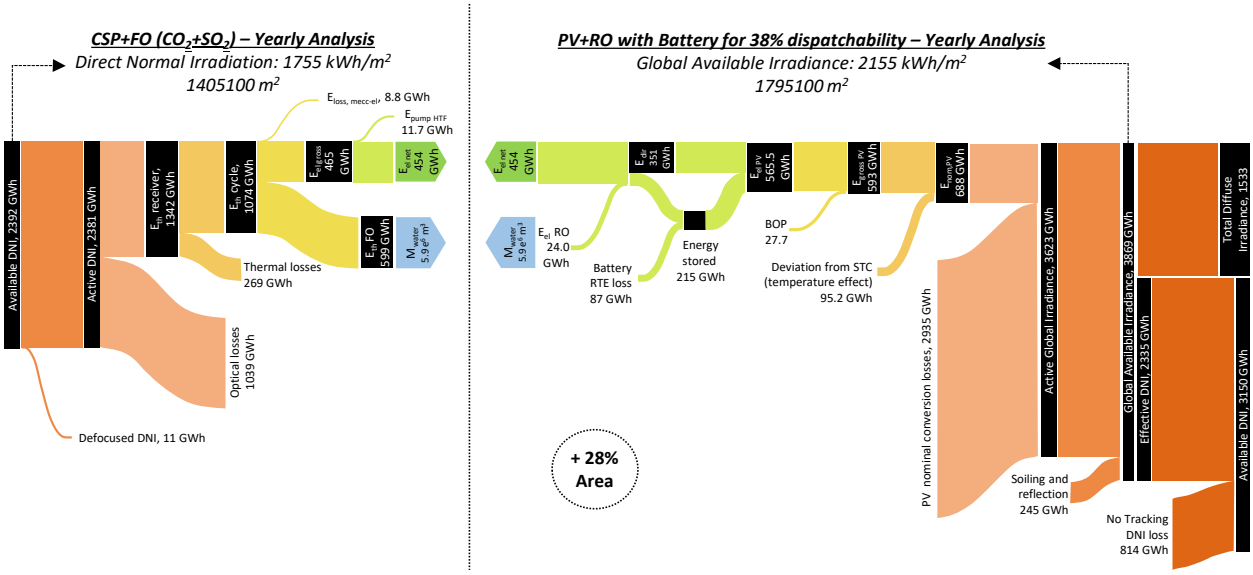

Figure 6. *Sankey diagram of the annual energy balance for the CSP+FO plant adopting CO_2+SO_2 mixture (left) and the reference case of PV+RO without battery (right).*

^ The resulting 28% of additional surface area of the PV field can be furtherly increased in conditions and location characterized by more abundant solar resources.

Conclusions

This work shows the performances of a forward osmosis desalination plant with innovative draw solute (PAGB2000) when coupled with a CSP plant. Two innovative power cycles based on transcritical CO_2 mixtures are considered and designed specifically to reach high electric efficiencies, when used in CSP plants. Their coupling with the FO plant allows for a large production of freshwater with almost negligible electric power auxiliary consumption (around 0.8% of the yearly energy produced by the cycle, a value compensated by the avoided parasitic consumption of the air-cooled condenser of the electric-only configuration).

The water production of the FO plant can be around 50% higher than the one adopting a more conventional desalination technology (MED) when applied to the same CSP plant and power cycles, with a specific thermal consumption of 100 kWh_{th}/m^3. When the innovative system is compared with a state-of-the-art PV+RO cogenerative system located in Dubai, and assuming the same yearly outputs of both energy and freshwater produced, the surface area of the PV plant results around + 28% higher than the surface area of the heliostats of the CSP plant.

Data availability statement

Data will be made available on request.

Author contributions

Ettore Morosini: Methodology, Software, Formal analysis, Investigation, Writing – original draft. **Igor Matteo Carraretto**: Methodology, Validation, Investigation, Writing – original draft. **Riccardo Simonetti**: Software, Formal analysis, Investigation. **Marco Binotti** Supervision,

Conceptualization and Writing – review. **Marco Astolfi**: Supervision, Investigation, Writing – original draft and Writing – review. **Giampaolo Manzolini**: Methodology, Conceptualization, Writing – review & editing, Supervision, Project administration, Funding acquisition.

Competing interests

The authors declare that they have no known competing financial interests or personal relationships that could have appeared to influence the work reported in this paper.

Funding

This project has received funding from the European Union's Horizon 2020 research and innovation program under grant agreement No. 101022686 (DESOLINATION).

References

[1] G. Manzolini *et al.*, "Adoption of CO2 blended with C6F6 as working fluid in CSP plants," in *AIP Conference Proceedings*, AIP Publishing, 2022., doi:10.1063/5.0086520.

[2] M. Doninelli *et al.*, "Thermal desalination from rejected heat of power cycles working with CO2-based working fluids in CSP application: a focus on the MED technology.," *Sustain. Energy Technol. Assessments*, vol. 60, 2023, doi:10.1016/j.seta.2023.103481.

[3] R. Colciaghi, R. Simonetti, L. Molinaroli, M. Binotti, and G. Manzolini, "Potentialities of thermal responsive polymer in forward osmosis (FO) process for water desalination," *Desalination*, vol. 519, no. September 2021, p. 115311, 2022, doi:10.1016/j.desal.2021.115311.

[4] G. Picotti, M. E. Cholette, F. Casella, M. Binotti, T. A. Steinberg, and G. Manzolini, "Dynamic thermal analysis of an external cylindrical receiver in an object-oriented modelling paradigm," in *AIP Conference Proceedings*, AIP Publishing, 2022., doi:10.1063/5.0085650.

[5] M. J. Wagner and T. Wendelin, "SolarPILOT: A power tower solar field layout and characterization tool," *Sol. Energy*, vol. 171, pp. 185–196, 2018, doi:10.1016/j.solener.2018.06.063.

[6] "Steel Tubes, n.d. Dimensions and weights of seamless tubes according to standard ASME B36.10M - Steel tube." https://www.steeltube.sk/sizes/dimensions-and-weights-of-seamless-tubes-according-to-standard-asme-b36-10m/

[7] E. Morosini, E. Villa, G. Quadrio, M. Binotti, and G. Manzolini, "Solar tower CSP plants with transcritical cycles based on CO2 mixtures: A sensitivity on storage and power block layouts," *Sol. Energy*, vol. 262, p. 111777, 2023, doi:10.1016/j.solener.2023.05.054.

[8] G. Gentile, G. Picotti, F. Casella, M. Binotti, M. E. Cholette, and G. Manzolini, "SolarReceiver2D: a Modelica Package for Dynamic Thermal Modelling of Central Receiver Systems," *IFAC-PapersOnLine*, vol. 55, no. 20, pp. 259–264, 2022, doi:10.1016/j.ifacol.2022.09.105.

[9] E. Morosini, G. Gentile, M. Binotti, and G. Manzolini, "Techno-economic assessment

of small-scale solar tower plants with modular billboard receivers and innovative power cycles," in *Journal of Physics: Conference Series*, IOP Publishing, 2022, p. 12109., doi:10.1088/1742-6596/2385/1/012109.

[10] G. Di Marcoberardino *et al.*, "Experimental characterisation of CO2 + C6F6 mixture: thermal stability and vapour liquid equilibrium test for its application in transcritical power cycle," *Appl. Therm. Eng.*, p. 118520, 2022, doi:10.1016/j.applthermaleng.2022.118520.

[11] E. Morosini, A. Ayub, G. di Marcoberardino, C. M. Invernizzi, P. Iora, and G. Manzolini, "Adoption of the CO2+ SO2 mixture as working fluid for transcritical cycles: A thermodynamic assessment with optimized equation of state," *Energy Convers. Manag.*, vol. 255, p. 115263, 2022, doi:10.1016/j.enconman.2022.115263.

[12] A. Inada, K. Yumiya, T. Takahashi, K. Kumagai, Y. Hashizume, and H. Matsuyama, "Development of thermoresponsive star oligomers with a glycerol backbone as the draw solute in forward osmosis process," *J. Memb. Sci.*, vol. 574, no. September 2018, pp. 147–153, 2019, doi:10.1016/j.memsci.2018.12.067.

[13] I. M. Carraretto *et al.*, "Characterization of the physical properties of the thermoresponsive block-copolymer PAGB2000 and numerical assessment of its potentialities in Forward Osmosis desalination," *Polym. Test.*, vol. 128, no. October, p. 108238, 2023, doi:10.1016/j.polymertesting.2023.108238.

[14] H. Truong-Ba, M. E. Cholette, G. Picotti, T. A. Steinberg, and G. Manzolini, "Sectorial reflectance-based cleaning policy of heliostats for Solar Tower power plants," *Renew. Energy*, vol. 166, pp. 176–189, 2020, doi:10.1016/j.renene.2020.11.129.

[15] M. Schimpe *et al.*, "Energy efficiency evaluation of a stationary lithium-ion battery container storage system via electro-thermal modeling and detailed component analysis," *Appl. Energy*, vol. 210, pp. 211–229, 2018, doi:10.1016/j.apenergy.2017.10.129.